



## Research article

# Reduction of polystyrene/polyurethane plastic wastes from the environment into binders for water-resistant emulsion paints

Sunday A. Osemeahon<sup>a</sup>, Ayodele Akinterinwa<sup>a,\*</sup>, Esther Fasina<sup>a</sup>,  
Fartisinha P. Andrew<sup>b</sup>, Muhammed H. Shagal<sup>a</sup>, Semiu A. Kareem<sup>c</sup>,  
Usaku Reuben<sup>b</sup>, Patience U. Onyebuchi<sup>b</sup>, Olubukola R. Adelagun<sup>d</sup>, David Esenowo<sup>a</sup>

<sup>a</sup> Department of Chemistry, Modibbo Adama University, PMB 2076, Yola, Nigeria

<sup>b</sup> Department of Science Laboratory Technology, Modibbo Adama University, PMB 2076, Yola, Nigeria

<sup>c</sup> Department of Chemical Engineering, Modibbo Adama University, PMB 2076, Yola, Nigeria

<sup>d</sup> Department of Chemistry, Federal University Wukari, PMB 1020, Taraba State, Nigeria

## ARTICLE INFO

## Keywords:

Composites  
Emulsion paints  
Recycled plastics  
Water-resistant coatings

## ABSTRACT

Waste management is fundamental to resource and environmental sustainability. Expanded polystyrene (EPS) and polyurethane (PU) waste plastics were recycled and applied as binder in emulsion paint formulation. The recycled polystyrene (rPS) and polyurethane (rPU) were blended into composite resins, where toluene was used as the solvent. The blends of rPS and rPU were optimized, while some physicochemical properties of the composite blends (rPS/PU) were evaluated. The results showed that the incorporation of rPU into rPS increased the viscosity (1818 mPa–3924 mPa), rate of gelation (dry-to-touch time: 15 min–0.25 min), moisture content (2.7%–8.1%), moisture uptake (3.2%–5.0%), solid content (48%–53.4%) and density (0.82 g/cm<sup>3</sup> to 1.050.82 g/cm<sup>3</sup>) of the rPS/PU composite resins. Characterization was carried out using Fourier transform infrared (FT-IR) spectroscopy, X-ray diffraction (XRD), thermogravimetric analysis (TGA), scanning electron microscope (SEM), and atomic force microscopy (AFM). The results summarily showed that there are interactions among the rPS and rPU molecules in the composite, where complimentary structural and morphological characteristics were also achieved. The composite resin also exhibited superior bond strength (0.5–4.24 Mpa) on wood, cast mortar, ceramic, and steel surfaces due to its stronger intra- and inter-surface interactions compared to the neat rPS resin. The composite resin was used as a binder in the formulation of emulsion paint. The paint exhibited stronger resistance to water, among other superior properties, when compared to the paints formulated using neat rPS and conventional polyvinyl acetate (PVA) resins. The reduction of plastic waste in this study holds potential for the production of highly water-resistant emulsion paint for outdoor and indoor applications.

## 1. Introduction

The phrase “waste to wealth” can only be sustained with advancements in research and innovations focused on novel recycling technology [1]. Waste plastics constitute a significant proportion of global solid waste pollution [2]. This pollution and its impacts

\* Corresponding author.

E-mail addresses: [ayoterinwa@mau.edu.ng](mailto:ayoterinwa@mau.edu.ng), [ayoterinwa@yahoo.com](mailto:ayoterinwa@yahoo.com) (A. Akinterinwa).

<https://doi.org/10.1016/j.heliyon.2024.e27868>

Received 9 October 2023; Received in revised form 8 February 2024; Accepted 7 March 2024

Available online 13 March 2024

2405-8440/© 2024 The Authors. Published by Elsevier Ltd. This is an open access article under the CC BY-NC license (<http://creativecommons.org/licenses/by-nc/4.0/>).

have continued to grow [3]. The trend of increasing plastic waste pollution may remain unbeatable as it is directly driven by the growth in global population and industrialization [4]. Waste and non-reusable plastic materials constitute environmental challenges that range from costly landfills to water and air pollution due to leaching and incineration [5]. The economic challenges of these issues lie in the cost of the final disposal of these materials from the environment via reduction or degradation to worthless and sometimes hazardous residues [6]. Middle- and low-income countries with inadequate waste management system and facilities have recently started facing the major impacts of solid waste, such as floods and environmental degradation. Therefore, profit-driven waste management and recycling come with general environmental conservation and other advantages, such as, saving the cost of nugatory disposal and disintegration and creating resourceful production channels. Advancements in solid waste recycling have also provided various efficient and low-cost materials for major construction and other engineering applications [7,8].

Polystyrene (PS) and polyurethane (PU) are among the plastic materials that significantly constitute solid waste [9]. Expanded polystyrene (EPS) is a low-additive grade of polystyrene materials that are majorly used in packaging and other structural applications [10]. EPS constitute the most voluminous polystyrene waste [11]. PS materials are basically thermoplastic materials. Hence, EPS has been reconstituted via various simple methods, including dissolution [12,13], precipitation [11], depolymerization [1], thermokinetic transformation, and extrusion (mechanical and thermal processes), and the resultant polymeric and functional materials have been reused in various structural and functional applications [10]. The dissolution of EPS has been described by the relative energy difference ( $RED > 1$ ) that correlates forces of interaction (nonpolar, dipolar, and hydrogen-bonding interactions) between PS and various solvents [14]. Dissolution and/or catalytic depolymerization of PS materials have been achieved using organic solvents. Osemeahon et al. [15] studied some physicochemical properties of resins prepared by dissolving EPS in different solvents, including toluene, gasoline, carbon tetrachloride, and chloroform. Gutierrez-Velasquez et al. [3] evaluated acetone, ethyl acetate, and their mixtures as solvents for EPS wastes. Toluene was also used in the catalytic depolymerization of various plastics, including polystyrene [16]. The dissolved PS typically produces polymeric resin, which can also dry to form adhesive and cohesive films [3]. These properties basically channeled the application of dissolved PS wastes towards different forms of coating applications, including paints [15] and asphalts [3]. Neat PS is hydrophobic. However, the dissolved PS resin (rPS) can form stable dispersion in water with the aid of the appropriate emulsifiers and mechanical agitation. This has been successfully incorporated into matrixes such as cement paste and mortar [18] and emulsion paints [19].

PU wastes are primarily from PU foams in general wastes from upholstery, utility materials (shoes, clothings, etc.), and many domestic and industrial structures and cushions [20,21]. PU materials are relatively biodegradable compared to PS [9]. However the process can be considered too slow for efficient PU waste management, while it may also generate another category of waste from the inorganic residue [21]. PU materials are thermoset materials, and this makes recycling complicated [21]. Some methods have been successfully used in the size reduction [21], degradation [22], or depolymerization [23] of PU materials. However, the resultant materials are typically non-polymeric, which limit or complicate their structural reuse. Nevertheless, a simpler method of recycling PU materials has been achieved by reducing PU materials to particles and using these as fillers in composite materials [24].

Composite materials are materials of interest, usually fabricated by incorporating different materials to produce new materials with unique and synergetic properties that may be desired for an application. The unique properties of the composite material are also expected to overcome the limitations that have been attributed to each of the components making up the composition of the composite [25]. Composite technology has been used to advance the potential of conventional materials and their structural and engineering applications [7,8]. Different methods have been used in the preparation of polymer-polymer composites, and the products have exhibited desired characteristics based on compatibility and unique morphologies due to  $\pi$ - $\pi$  and other molecular interactions [17, 26–29].

The incorporation of recycled polymers in coatings is growing among the possible end applications [30]. EPS was also dissolved with different mixtures of acetone and ethyl acetate, and the resultant materials were studied to optimize their applications in asphalt coating [3]. Godinho et al. [23] recycled PU materials via depolymerization in an acidolysis reaction using dicarboxylic acid, and the polyol-rich product was further reacted with isocyanate to produce the rPU coating resin. A superhydrophobic coating was formulated by dispersing polytetrafluoroethylene powder in a solution of rPS [29]. Güçlü [31], prepared water-reducible alkyd resins by using the water-soluble and insoluble fractions of the depolymerization product obtained after simultaneous glycolysis and hydrolysis of PET waste. PET has also been depolymerized and been chemically transformed into new polymers with mainly carboxylic end-groups. This was further transformed into polyester, which was used in the production of powder coatings [32]. The rPS obtained by dissolving EPS waste has been used as a binder in the formulation of organic solvent-based paints [33,34]. However, the products have drawbacks such as moisture trapping (in voids and pores created by solvent evaporation), film brittleness and weatherability failure, slow drying time, and environmental impact due to large amounts of volatile organic solvent released from the painted surfaces [17,33,34]. These shortcomings necessitate modifications to the rPS resin to improve its properties and also enhance stable dispersion in water for the formulation of a more eco-friendly water-based (emulsion) paint. In the previous study, EPS dissolved in gasoline was blended with different derivatives of urea formaldehyde resins to develop a copolymer resin that can be used as a binder for emulsion paints [17,19, 35]. The studies achieved excellent dispersion of the copolymer resins in water. However, the product exhibited limitations in terms of poor mechanical properties, moisture uptake, and hazardous formaldehyde emissions. The limitations are due to the intrinsic properties of the thermosetting urea formaldehyde resin derivatives (solubility in water and brittleness'), at the optimal fractions in the copolymer resins [17,19,35]. Further studies on the incorporation of stable hydrophilic resins or particles in the rPS hold potential for the development of a low-cost and eco-friendly emulsion paint binder with improved properties for stable and efficient application.

To the best of our knowledge, no work is available in the literature on the preparation of recycled polystyrene (EPS) and polyurethane composites, as well as studies on their characterization and applications as water-based paint binders. In this study, PS and PU plastic wastes were reduced to resins and composite resins, which were comprehensively characterized as binders for water-

resistant emulsion paint. The binders were further used in the formulation of emulsion paints. The significance of this study lies in the low-cost production and characterization of essential products for improved domestic and industrial applications from recycled waste materials.

## 2. Materials and methods

### 2.1. Materials

EPS waste (Fig. 1a) was picked from the garbage bin and cleaned thoroughly to remove all extraneous materials from it. Rigid polyurethane material (Fig. 1b) was removed from a disposed shoe sole. The toluene used was of synthesis grade (Sigma-Aldrich, 99.8% purity). Epoxy glue was from a local supermarket, and paint chemical and additives were purchased from a local chemical store.

### 2.2. Methods

#### 2.2.1. Preparation of rPS and rPS/PU composite

rPS resin was prepared by dissolving 30 g of EPS in 100 ml of toluene. After the dissolution of EPS, the resin formed was stirred at low speed in a closed container for 30 min. The rPU suspension was prepared by reducing the PU solid waste (2 g) in toluene (20 ml) by stirring for 10 min (or until complete suspension at room temperature) using a mechanical stirrer. The rPS/PU composites were prepared and optimized by blending rPS resin with the rPU suspension in different proportions, as shown in Table 1. The composite was stirred in a closed container using a mechanical stirrer at low speed for 30 min.

#### 2.2.2. Physicochemical analyses rPS and rPS/PU composite

Viscosity was determined at  $27 \pm 2$  °C using a Brookfield viscometer CAP 2000 based on ASTM D4287/ISO 2884. Resin was spread on a glass slide to produce about 0.45 mm of thickness, and the gel time was determined from dry-to-touch time according to standard methods (ASTM D1640). The moisture content of the resins was determined using a Karl-Fischer titrator instrument (MA101 C). Tetrahydrofuran (50 ml) was initially added to the titrator, and the water content was completely neutralized with the K-F reagent. Afterwards, resin (50 mg) was added to the THF as a diluent, stirred for about 10 min, and then neutralized completely by the K-F reagent. The moisture content computed by the instrument was recorded. Moisture uptake of film was determined gravimetrically using the Moisture Sorption Analyser IGAsorp (Hiden Isochema Ltd.), with relative humidity ranging from about 0% to 95% as described by Ref. [36]. Density and the solid content (non-volatile content at 120 °C) were determined according to ASTM D792 and ASTM D2369 standard methods. All analyses were carried out in triplicate.

#### 2.2.3. Characterization of rPS and rPS/PU composite

rPS and rPS/PU film of about 1 mm thickness cast on a clean glass slide were allowed to dry-through and used for instrumental characterization. The chemical functionality of the materials was investigated using Fourier transform infrared (FTIR) spectroscopy. The FTIR analysis was carried out using an Agilent (Cary 630) spectrometer operated at  $8 \text{ cm}^{-1}$  resolutions, a spectra range of  $4000\text{--}650 \text{ cm}^{-1}$ , and 30 scans per second.

The morphological characteristics of the materials were evaluated using X-ray diffraction (XRD). XRD analysis was carried out using a Shimadzu XRD-6000 diffractometer operated at 40 kV and 30 mV. The scanning range of  $2\theta$  was between 2.0 and 65.0, the scan speed was  $2^\circ 2\theta/\text{min}$ , and the receiving slit width was 0.30 mm.

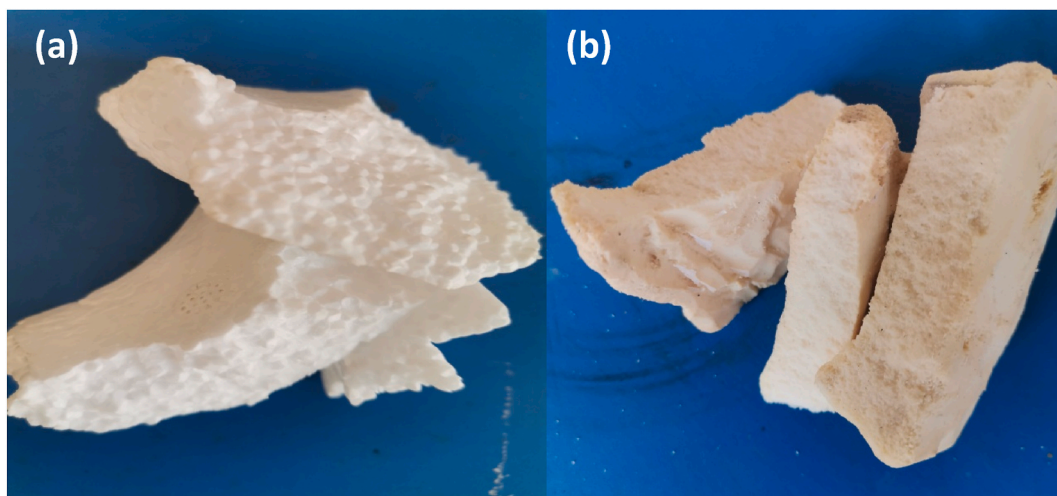


Fig. 1. Pieces of waste EPS (a) and rigid polyurethane (b) materials.

**Table 1**  
Preparation of blends of rPS and rPU.

Sample	C1	C2	C3	C4
rPS-rPU blended (ml)	100–5	100–7	100–11	100–15
Ratio	1:0.05	1:0.07	1:0.11	1:0.15

A Phenom ProX scanning electron microscope operated at an acceleration voltage of 15 kV, was used to depict the micrograph of the materials.

The thermal stability of the materials was studied using thermogravimetric analysis (TGA). TGA was performed with the SDT Q600 V20.9 Build 20 instrument. The temperature of the analysis started from 25 °C to 900 °C within an inert nitrogen atmosphere with a heating rate of 10 °C min<sup>-1</sup>.

A 3D nanoscale micrograph of materials was depicted using the atomic force microscopy (AFM). This was performed using Nanosurf Naio AFM.

#### 2.2.4. Bond strength analyses of rPS and rPS/PU composite

Bond strength on different substrate surfaces, including wood, ceramic, steel, and cast mortar (a mixture of cement, sand, and water), was carried out at about 27 ± 2 °C, according to Ref. [37], as shown in the experimental assembly illustrated in Fig. 2. Coating (rPS and rPS/PU) about 2 ± 0.2 mm thick was applied to a piece of substrate (fabricated to about 25 mm in diameter of the steel sliders) and allowed to dry-through (within 5–8 h). Epoxy glue (2 ± 0.2 mm) was used to glue the coated and non-coated surfaces of the substrate to the steel slide and left for 24 h to cure completely (our prior experiment confirmed that the epoxy glue is suitable and stable because the bond strength is much higher on the selected surfaces). Afterwards, the assembly was mounted on a universal stretching machine (Instron Microtester 5848) for a tensile test. The maximum loading at substrate-coating interface rupture was recorded. Coating bond strength was calculated using equation (1).

$$f_b = \frac{F}{A} \quad 1$$

Where  $f_b$  is the bond strength (MPa), F is the maximum loading at substrate-coating interface rupture (N), and S is the area of substrate (mm<sup>2</sup>).

The effect of waste/composite concentration on bond strength was also studied by varying the concentration from 5 to 25 % w/v in the solvent.

#### 2.2.5. Paint formulation

Paint formulation was carried out using conventional methods as described in the previous study [19], with minor modifications. The sequential addition and mixing of the paint component materials are highlighted in Table 2. Mixing was carried out in a transparent container while using a mechanical stirrer tuned from medium to high speed. Mixing was stopped at about 15–20 min, after homogeneous and consistent mixtures were obtained at every stage of the paint formulation process.

#### 2.2.6. Paint tests

A digital pH meter (Hanna instrument) was used to measure the pH of paint products. Viscosity, density, and drying time tests were carried out using the same methods as for the binder resins. The washability cycles evaluation was carried out using the Biuged BGD 526 Wet Abrasion Scrub Tester. Opacity, adhesion, tackiness, chemical resistance (for 12 h in aqueous solution), and stability (for 4 months) tests were carried out as described in the previous study [19]. The static immersion test was carried out according to the method described by Yew et al. [38] over 7 days in distilled water. A complementary immersion-water-resistant test was carried out using an in-house technique where a cast rectangular cement mortar (substrate) was gently dipped into the paint container to get evenly coated, then pulled out and set to dry completely for 24 h. The dried painted substrate was then immersed gently in distilled water for 14 days in a transparent container where frequent virtual observation was made. All test data were recorded as the mean of triplicate determinations, and all tests were carried out at room temperature (27 ± 2 °C).

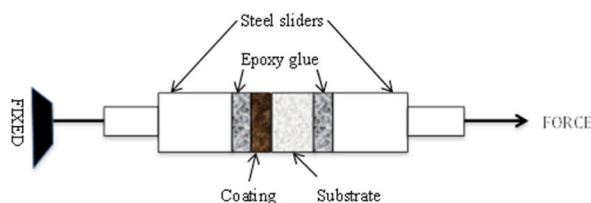


**Fig. 2.** Assembly of materials for coating bond strength test.

**Table 2**  
Paint formulation recipe and stages.

Stages	Material	Quantity (g)
First Stage (Wetting and dispersion) 15–20 min	Water	185.00
	Anti-foam	0.20
	Drier	0.20
	Calgon	1.16
	Genepour	1.16
	Bermocoll	2.50
	Troystan	1.14
	Dispersant	0.20
	Butanol	5.00
	Ammonia	0.54
Second Stage (Millbase) 15–20 min	TiO <sub>2</sub>	50.00
	Al <sub>2</sub> SiO <sub>3</sub>	11.20
	Na <sub>2</sub> CO <sub>3</sub>	0.58
	Kaolin	2.52
	CaCO <sub>3</sub>	123.00
Third Stage (Letdown) 15–20 min	Binder	100.00
	Water	15.00
	Dispersant	0.20
	Nicofoam	0.20
	Anti-skining agent	0.20
<b>Total</b>		<b>500</b>

### 3. Results and discussion

While the EPS material dissolved to form a homogeneous-phase resin, the rigid PU material only disintegrated to form a dispersion of white, soft, solid particles in toluene. The visual presentation of the rPS, rPU, and the different proportions of rPS/PU composite resins were presented in Fig. 3. Homogeneity and consistency visually decreased with an increase in the amount of rPU incorporated in the rPS resin. At higher rPU proportions, larger lumps were formed, which virtually created inconsistency and disrupt homogeneity in the composite resins. This may decrease the workability of the composites with a higher proportion of rPU suspension.

Fig. 4 presents the results of some physicochemical properties of rPS and the rPS/PU composites. The results of viscosity and gel time (dry-to-touch) of rPS and rPU/PS composites were presented in Fig. 4a. Viscosity increased (1818–3924 cP from rPS to C4 respectively) while the gel time decreased (15–0.25 min from rPS to C4 respectively) with the incorporation and increase in rPU in rPS. This indicated molecular interactions between the rPS and rPU particles, which increased molecular weight and cumulatively reduced the mobility of the macromolecules in the composite [23]. This effect also showed that the rPS and rPU materials are compactible and that the incorporation of rPU particles alters the microstructure of the rPU material [39]. Ramos Olmos has also shown that reactive additives increase the viscosity of polystyrene solutions [40]. Fig. 4b presents the moisture content of the materials and the moisture uptake by the materials. The moisture content in rPS can be attributed to moisture trapped within the pores in the resin film [3]. Moisture content increased with an increase in rPU content. This showed that the rPU particles impact hydrophilic functionality (compatibility with water) in the composite. This effect may serve as the basis for using the composite as a binder in emulsion coatings. Moisture uptake by composites showed a lower trend compared to the results of the moisture content. This showed different kinetics of moisture loss due to drying and moisture re-absorption on the composite. The lower water uptake trend signals the ability of the composite film to continue structural transformations that increase its resistance to moisture as it ages. The density and solid content of the materials increased with similar trends (Fig. 4c), as expected for dense fillers in composites. Ramos-Olmos et al. [40] also reported an increase in viscosity with solid content when polyethylene glycol was increased in a polymer composite of polystyrene. C2 was selected for further instrumental characterization based on its optimum physicochemical properties.

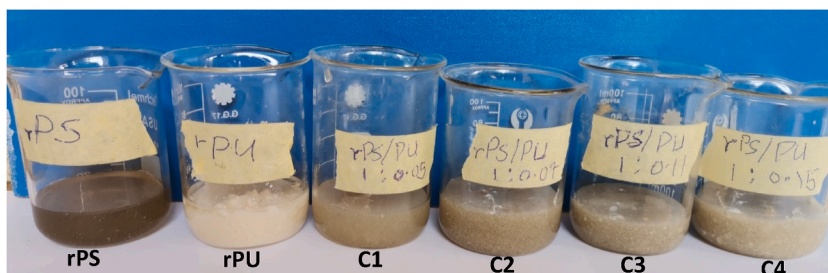


**Fig. 3.** Visual presentation of rPS, rPU, and rPS/PU composites in different (C1–C4) proportions.

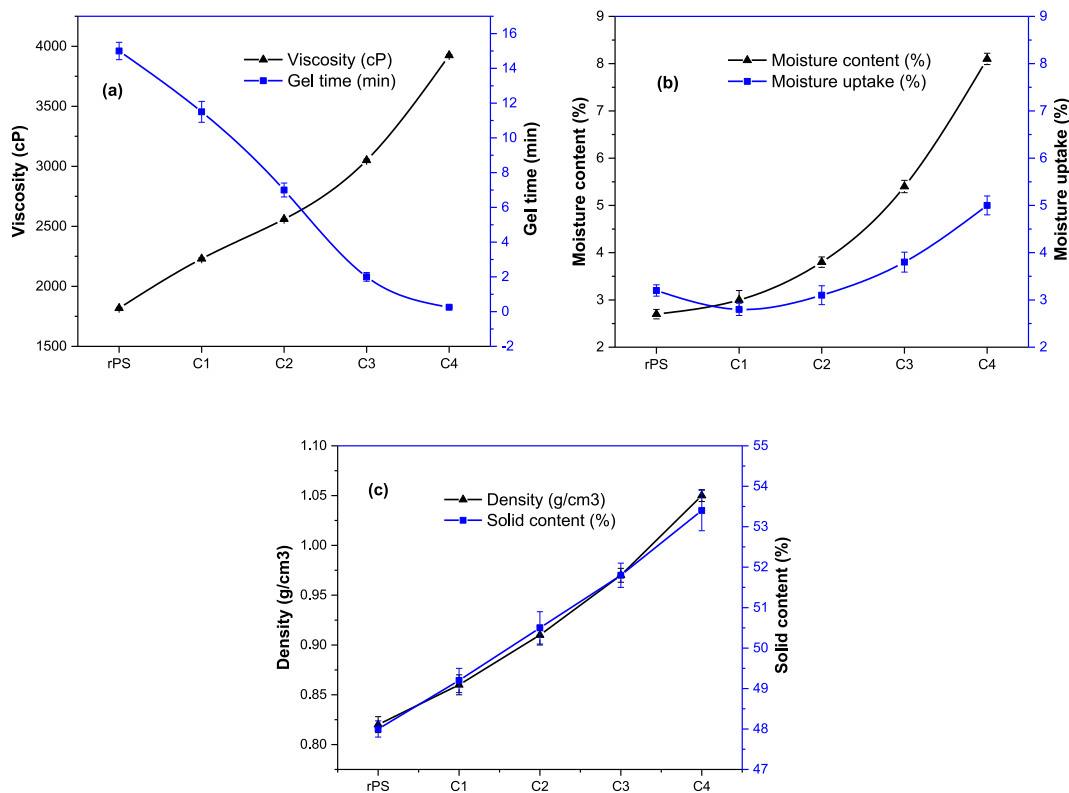


Fig. 4. Viscosity and gel time (dry-to-touch) (a), moisture content and moisture uptake (b), and the density and solid content of rPS and the composites.

### 3.1. Fourier transform infrared (FTIR) spectroscopy

Fig. 5 shows the FTIR spectra of the rPS and rPS/PU composites. rPS spectra show major similarities to spectra available in the literature [12,13,17,26,41]. The peaks that are common to both spectra within  $3200\text{--}2800\text{ cm}^{-1}$ ,  $1700\text{--}1300\text{ cm}^{-1}$ , and  $1200\text{--}600\text{ cm}^{-1}$  can be attributed to aliphatic/aromatic C–H stretching, aliphatic C–H bending/C=C stretching/aromatic C=C–C stretching, and aromatic C–H/C–Substituent bending vibrations (on monosubstituted benzene rings), respectively. The peaks at  $906.7\text{ cm}^{-1}$  and  $842.4\text{ cm}^{-1}$  are attributed to the amorphous phase due to atactic PS [12]. These characteristic peaks indicated the presence of

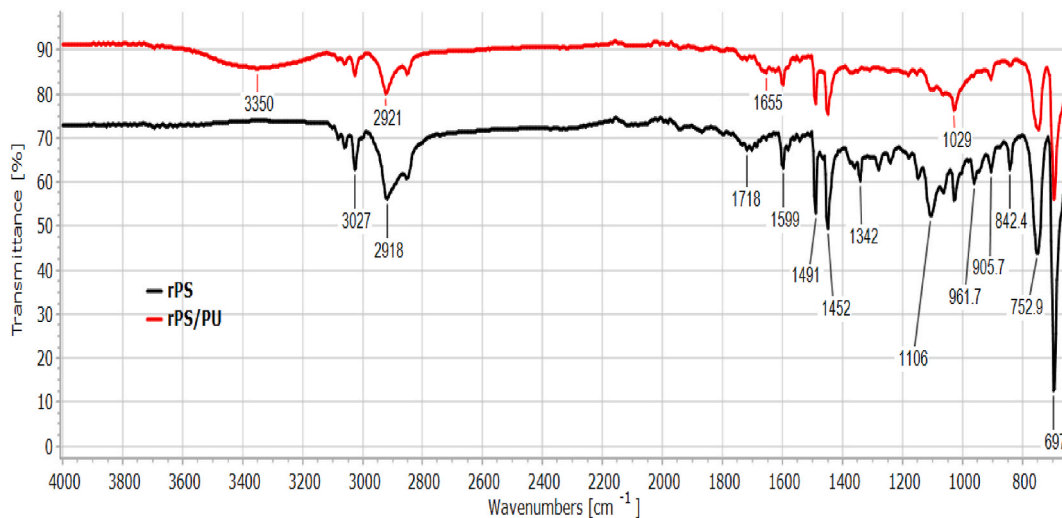


Fig. 5. FTIR spectra of rPS and rPS/PU.

polystyrene fractions in both materials. The unique peaks at  $1342\text{ cm}^{-1}$  and  $961.7\text{ cm}^{-1}$  on the rPS spectra can be specifically attributed to the  $\alpha$ -carbon C–H bending and the vinyl C–H bending vibrations on styrene molecules in the resin, respectively. The presence of styrene in rPS can be attributed to residual styrene in the Styrofoam and partial degradation of polystyrene in the solvent [16]. The rPS/PU spectra showed relative changes in intensity and the disappearance of some peaks compared to rPS. The spectra also showed new peaks at  $3350\text{ cm}^{-1}$  and  $1655\text{ cm}^{-1}$ , which were attributed to N–H stretching and  $\text{C}(=\text{O})\text{--N}$  functional group vibrations, respectively. These peaks indicated the amine and amide groups of the rPU in the composite [42]. The disappearance of peaks on rPS/PU spectra (particularly  $1342\text{ cm}^{-1}$  and  $961.7\text{ cm}^{-1}$  on rPS) indicated that rPU interacts with styrene molecules and reduces the amount of styrene in the composite. The changes in peak intensities can be attributed to changes in the conformation of polystyrene molecules in the composite due to the incorporation of rPU. The grafting reaction of styrene molecules with rPU particles in Scheme 1, as similarly proposed by Jeong et al. [27], is expected to enhance the stable dispersion of rPU particles in the rPS/PU composite.

### 3.1.1. X-ray diffraction (XRD) analysis

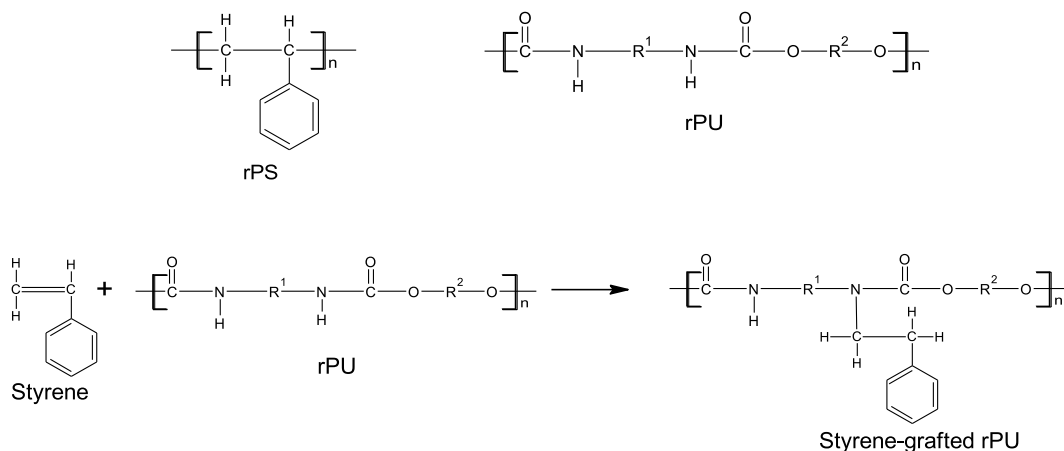
Fig. 6 presents the XRD spectra of rPU and rPS/PU composite films. The position of the single broad reflection peak on the rPS spectra was at  $18.84^\circ$  on the  $2\theta$  scale, and this also corresponds to an interplanar distance of  $4.481\text{ \AA}$ . The spectra agree with the semi-crystalline structure of polystyrene [11,43]. The rPS/PU spectra also showed a single broad peak at  $16.62^\circ$  on the  $2\theta$  scale with an interplanar spacing of  $5.41\text{ \AA}$ . The rPS/PU crystalline peak ( $16.62^\circ$ ) is less than the range of characteristic  $2\theta$  angles ( $18\text{--}22^\circ$ ) that have been reported for both polystyrene and polyurethane materials [11,42,43]. This indicated the formation of a unique crystalline lattice due to the new products from the chemical interactions between component materials (Scheme 1). The single broad peak on the composite resin film indicated the formation of a homogenous microstructure resin film [42]. The composite resin also showed significant morphological modification, with a reduction in the crystallinity of the composite ( $19.69\%$ ) compared to the rPS resin ( $39.93\%$ ). The increase in interplanar spacing in the rPS/PU composite indicated lattice strains and the disruption of crystallinity structures in the composite resin compared to rPS. The formation of new material phase and the change in the morphology of the composite resin are also supported by the functional characterization (FTIR analysis) of the resin.

### 3.1.2. Thermogravimetric analysis (TGA)

Fig. 7 presents the results of the thermogravimetric analysis (TGA) of rPS and rPS/PU, which depicts the thermal stability of the materials. The TGA result showed a remarkable change in the thermal degradation of rPS compared to the rPS/PU composite, and the difference was initially detected at about  $123^\circ\text{C}$ . The rPS thermogram showed a loss of about  $4.5\%$  of volatile materials before the onset of major degradation of polystyrene at  $220^\circ\text{C}$ , followed by the final degradation of residual materials at  $499^\circ\text{C}$ . rPU showed similar degradation steps; however, the  $220^\circ\text{C}$  onset degradation temperature recorded in this study is lower compared to the popular range ( $290\text{--}350^\circ\text{C}$ ) in the literature [3,11,12,26]. This may be attributed to the partial degradation or depolymerization of PS in the rPS [44]. The rPS/PU thermogram showed more degradation steps than rPS. The first slight degradation step onset at  $123^\circ\text{C}$  can be attributed to the second phase of volatile materials released from the rPU, which is the second component material in the composite. The second degradation step onset at  $301^\circ\text{C}$  can be attributed to the PU segments in the composite [23,45]. The emergence of the third step at  $384^\circ\text{C}$  can be attributed to the new PU-styrene products in the composite [27]. The TGA result ultimately showed that rPS/PU exhibits higher thermal stability compared to rPS. This property is also expected to improve the resistance to flame and other thermal deformation of the paint formulated using the rPS/PU composite resin as the binder.

### 3.1.3. Scanning electron microscope (SEM) analysis

Fig. 8 depicts the micrograph of the surface morphology of the rPS and rPS/PU composites. The result showed lateral orientation on the surface of the rPS film (Fig. 8a), with different sizes of pores and voids which can be attributed to the spaces created by bubbled gas during the drying process [3]. The rPS/PU composite film also exhibits lateral orientation on the surface. However, there were no void



**Scheme 1.** General structure of polystyrene (rPS), polyurethane (rPU), and a graft reaction of styrene and rPU.

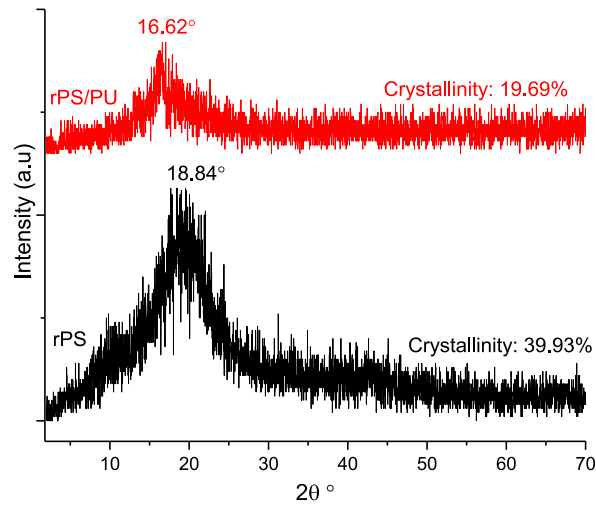


Fig. 6. XRD spectra of rPS and rPS/PU.

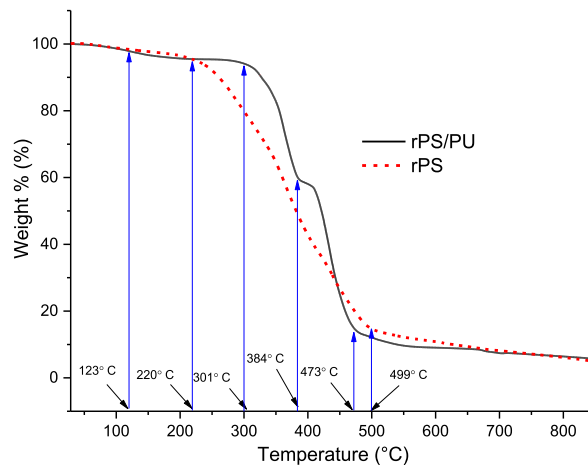


Fig. 7. TGA graph of rPS and rPS/PU composite.

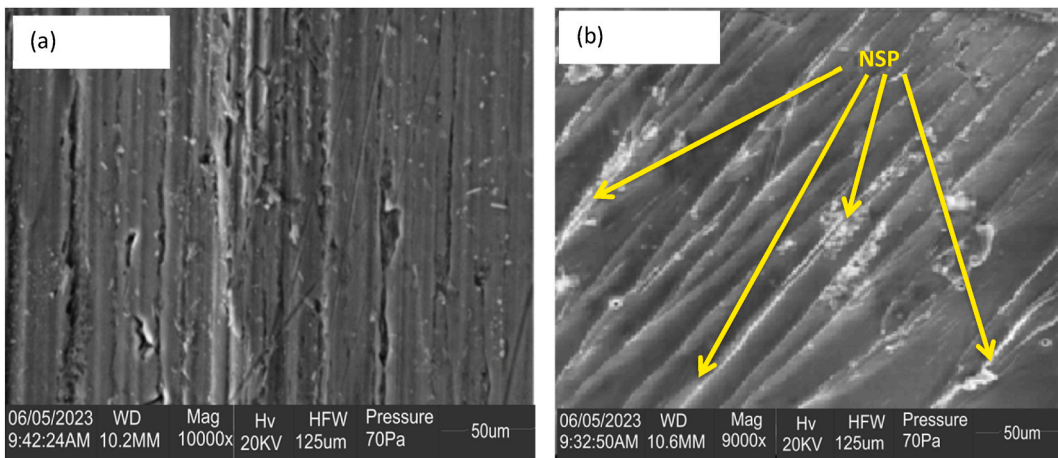


Fig. 8. SEM images of (a), rPS and (b), rPS/PU.

spaces, which indicated that rPU particles controlled the drying process to maintain structural compactness. The micrograph of the rPS/PU composite (Fig. 8b), also showed patches that correspond to new structural phases (NSP) of materials that preferentially filled the void spaces and are also randomly distributed across the direction of orientation on the surface of the film. The NSP serves as a filler and reinforcer in the composite film, which further supports the results obtained from the thermal stability of the composite. The NSP on the rPS/PU can be attributed to rPU particles and the new product from the rPU-Styrene interactions [27,45,46].

### 3.1.4. Atomic force microscopy (AFM) analysis

AFM produced the 50  $\mu\text{m}$  by 50  $\mu\text{m}$  topographic 3D images of rPS and rPS/PU composite, as shown in Fig. 9 (a) and 9(b) respectively. The gray-colored openings on the micrograph images represent the pore and void spaces. The substantial reduction in pores and voids clearly showed that the surface morphology of the rPS film was remarkably altered due to the incorporation of rPU. The 91.8 nm peak-to-valley height on rPS was reduced to 2.75 nm on rPS/PU. This indicated that rPU particles and the resultant PU-styrene derivative preferentially take forms that fill the valleys (pores) on the rPS. Similar effect was reported by Ref. [28]. The nano-scale modification reduced porosity and increased surface homogeneity (reduced roughness) of the rPS/PU composite compared to the rPS resin film. This result also complements the results obtained from the SEM micrograph images. The reduction in surface roughness due to the deformation of soft filler particles in the composite films is expected to enhance both the adhesive and cohesive properties of the composite film [28].

### 3.1.5. Bond strength of rPS and rPS/PU on different material surfaces

The bond strengths of rPS and rPS/PU (C2) at different concentrations in toluene were studied on different substrates, as presented in Fig. 10a-d. The results showed that rPS/PU has higher bond strength than rPS on all the surfaces that were studied. This property can be attributed to the reduction in surface roughness of the rPS/PU observed on the AFM micrograph. A reduction in surface roughness is expected to improve the wettability of rPS/PU compared to rPS. The higher bond strength of the rPS/PU resin can also be attributed to higher hydrogen bonding and other molecular interactions or bonding between the substrate molecules and the electron rich functional groups (such as carboxyl C=O and amine N-H) introduced into the composite due to rPU [47]. The results also showed that the bond strength increased with the amount of recycled materials in the solvent. The highest bond strength of rPS/PU on different substrates follows the order: wood > cast mortar > ceramic > steel.

### 3.1.6. Properties of paints formulated using rPS, rPS/PU, and conventional polyvinyl acetate (PVA) resins

The paints formulated were applied and completely dried on a cast mortar (Fig. 11a). Visually, the PVA paint exhibited a bright white color (of the  $\text{CaCO}_3$  particles), while the brightness was reduced in the rPS paint and further reduced towards an off-white color in the rPS/PU paint. This can be attributed to the colors of the binders, ranging from white (PVA), to golden brown (rPS), to dark (rPS/PU) color (S1). The rPS/PU paint exhibited the best opacity. This is due to the filling effects of the PU particles, which may reduce the amount of pigment required in the paint. The physical properties of the paints, as presented in Table 3, exhibit some unique characteristics of binders reported earlier in this study. rPS/PU paint exhibited outstanding properties with higher viscosity and density (better molecular and structural aggregation), washability cycles, better flexibility, and faster drying time than rPS, which culminated in a better product [29].

### 3.1.7. Immersion (water-resistant) and chemical resistant tests

The visual effect of water immersion of paint coated on cast mortar was presented before immersion (Fig. 11a) and after immersion in tap water for 14 days (Fig. 11b). The results showed that both rPS and rPS/PU paints were resistant to blistering while the PVA paint failed. The water-proof effect showed that the strong water-resistance characteristic of the rPS was retained in the rPS/PU composite resin. Therefore, the emulsion paints formulated using the recycled plastics' resins have potential for applications on submersible materials. The results of the paint film static immersion test showed that the PVA paint film is the least stable in water (Fig. 11c). The PVA paint film exhibited the highest (4.61 %) and most rapid weight loss till day 5, while the rPS paint lost less weight (2.21 %) within the same period. The rPS/PU paint film initially exhibited a rapid loss in weight (about 2.24 % at day 3), and further exhibited a slightly reversed weight gain from day 4. The weight gain can be attributed to the re-adsorption of substances in the water by the urethane components in the rPS/PU [48]. This dynamic (porous) property may also create inert moisture transport channels, which will limit the deteriorative trapping of water molecules within the paint film and within the interface between the paint film and the substrate, thereby preventing paint failure in water or a humid environment. This controlled moisture transport technique has been successfully used in coating materials for food packaging [49].

Table 4 presents the stability/resistance of the coated paint films in typical aqueous solutions. rPS and rPS/PU paints exhibited better resistance to chemical agents than PVA paints in the aqueous solutions. This may be attributed to PS's intrinsic chemical resistance properties as established in the literature [29]. rPS/PU paint exhibited higher resistance/stability in 0.1 M acid solution than rPS paint. This may be attributed to increase in wear resistance and plasticization of the polyurethane particles in the acidic medium which serves as a reinforcement which has further stabilized the paint in the acidic medium [50].

## 4. Conclusion

(1) The incorporation of rPU suspension into the rPS resin produced a colloidal composite resin with stable dispersion. (2) The rPU particles serve as fillers and enhance the mechanical (flexibility) and physicochemical (drying time, resistance to moisture absorption) qualities of the composite resin. (3) Functional characterization of the composite indicated chemical interactions between rPU

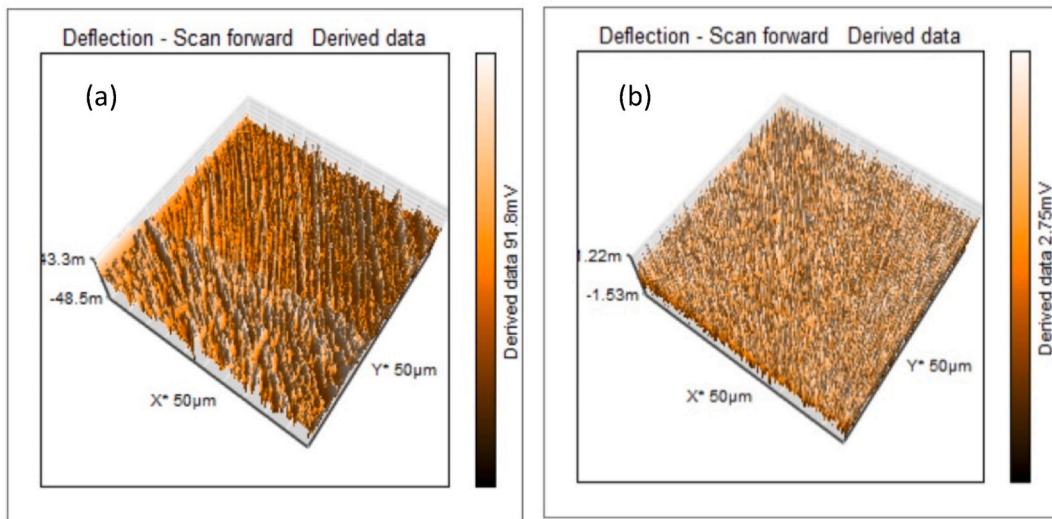


Fig. 9. AFM images of (a) rPS and (b) rPU/PS.

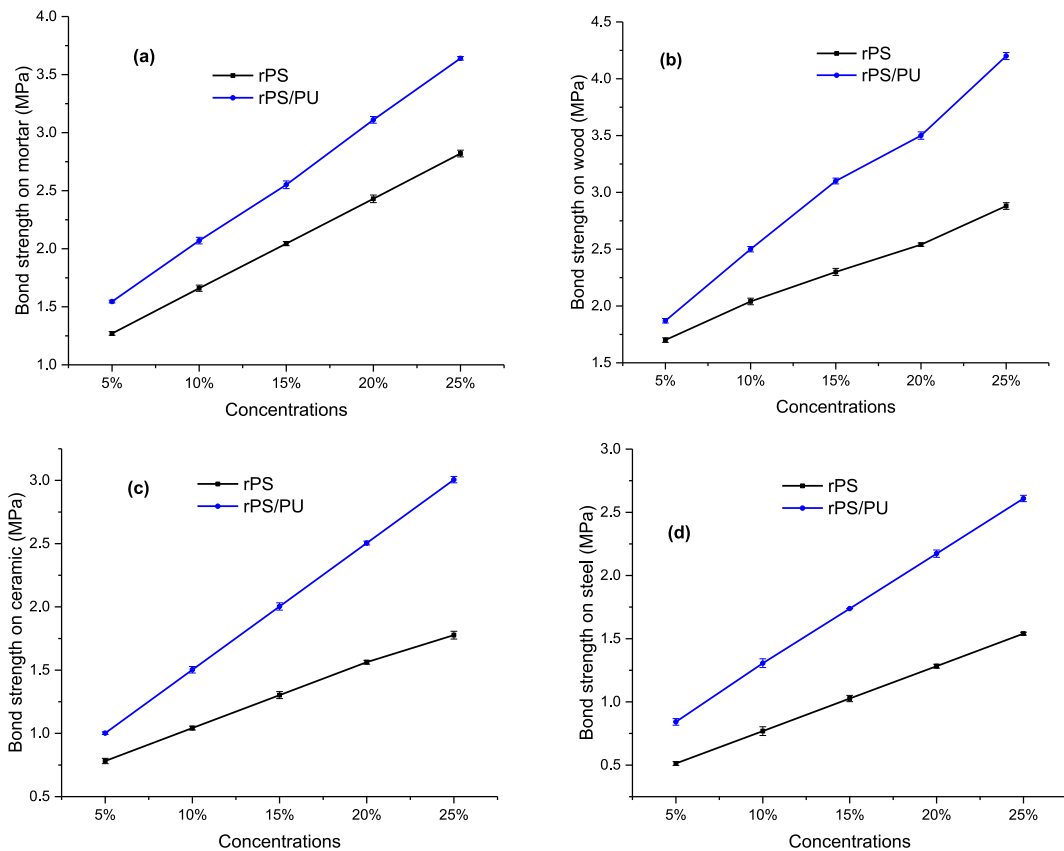
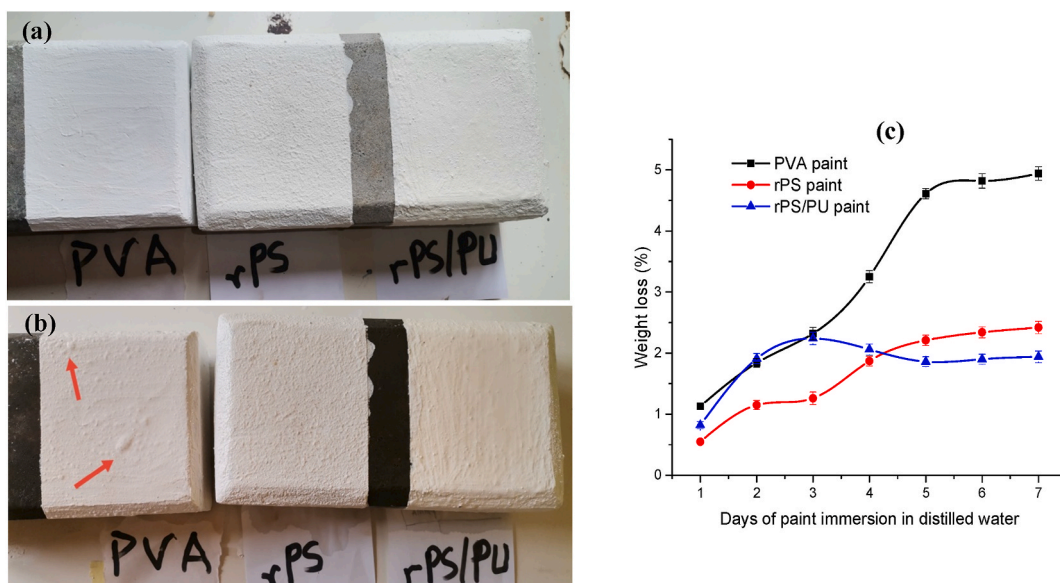


Fig. 10. Bond strength of rPS and rPS/PU on (a) cast mortar, (b) wood (c) ceramic and (d) steel surfaces.

particles and the rPS resin. The chemical interaction demonstrated the rPU particles' stability and complementary functionality within the composite resin. (4) The composite resin also exhibited microstructural and morphological characteristics that support the observed improvements in its physicochemical properties compared to the neat rPS resin. (5) The rPU in the composite resin impacts the carbonyl (C=O) and amine (N-H) functional groups. The hydrogen bonding characteristics of these functional groups improved the composite resin adhesion as well as its dispersion in water. (6) The emulsion paint formulated using the composite resin exhibited



**Fig. 11.** PVA, rPS and rPS/PU paints coated on cast mortar (a) before immersion in distilled water and (b) after immersion for 14 days. (c) Static immersion tests in distilled water.

**Table 3**

Physical properties of paints formulated using PVA, rPS, and rPS/PU as binder.

Property	PVA	rPS	rPS/PU
pH	8.2	8.6	9.1
Adhesion (on cast mortar surface)	Passed	Passed	Passed
Viscosity (Poise)	8.6 ± 0.07	18.1 ± 0.11	24.6 ± 0.20
Density (g/cm <sup>3</sup> )	1.131 ± 0.021	1.241 ± 0.002	1.357 ± 0.014
Washability Cycles	15	20	24
Opacity	Passed	Passed	Passed
Flexibility	Passed	Failed	Passed
Tackiness	Passed	Passed	Passed
Stability (4 months)	Passed	Passed	Passed
Drying time (min at 27 ± 2 °C)			
Dry to touch	50 ± 2.5	31 ± 1.0	19 ± 2.0
Dry to hard	85 ± 1.5	58 ± 3.0	44 ± 2.5

**Table 4**

Chemical inertness of PVA, rPS and rPS/PU paints.

Chemical solutions	PVA	rPS	rPS/PU
NaCl solution (5%)	Passed	Passed	Passed
H <sub>2</sub> SO <sub>4</sub> solution			
0.1 M	Failed	Failed	Passed
pH 1	Failed	Passed	Passed
pH 3	Passed	Passed	Passed
pH 5	Passed	Passed	Passed
NaOH solution			
pH 8	Passed	Passed	Passed
pH 10	Passed	Passed	Passed
pH 12	Failed	Passed	Passed
0.1 M	Failed	Passed	Passed

Pass: No visually observable effects; Fail: shrinks/blisters/cracks/peels was visually observed.

outstanding properties, including excellent water resistance. The new rPS/PU composite resin prepared in this study from waste plastics was achieved using simple techniques. Evaluation and characterization of the composite resin showed its potential as a multipurpose adhesive and as a binder for water-resistant emulsion paints. The study establishes sustainability through waste management and valorisation, as well as resource conservation.

## Data availability statement

Data associated with this study has not been deposited into a publicly available repository. Data will be made available on request.

## CRediT authorship contribution statement

**Sunday A. Osemeahon (SAO):** Conceptualization, Methodology, Funding acquisition, Project supervision, Administration, Review, Formal analyses, Manuscript editing. **Ayodele Akinterinwa (AA):** Methodology, Formal analysis, Data collection, Curation, Analyses, Writing - review and editing of the final manuscript. **Esther Fasina (EF):** Methodology, Data collection, Formal analyses. **Fartisincha P. Andrew (FPA):** Funding acquisition, Methodology, Data collection, Project supervision Reviews. **Mohammed H. Shagal (MHS):** Funding acquisition, Methodology, Data collection, Project supervision Reviews. **Semiu A. Kareem (SAK):** Funding acquisition, Methodology, Data collection, Project supervision Reviews. **Usaku Reuben (UR):** Funding acquisition, Methodology, Data collection, Project supervision Reviews. **Patience U. Onyebuchi (PUO):** Funding acquisition, Methodology, Data collection, Project supervision Reviews. **Olubukola R. Adelagun (ORA):** Funding acquisition, Methodology, Data collection, Project supervision Reviews. **David Esenowo (DE):** Methodology, Data collection, Formal analyses.

## Declaration of competing interest

The authors declare the following financial interests/personal relationships which may be considered as potential competing interests: Prof. S.A. Osemeahon reports financial support was provided by Tertiary Education Trust Fund. If there are other authors, they declare that they have no known competing financial interests or personal relationships that could have appeared to influence the work reported in this paper.

## Acknowledgements

This research work was funded by Tertiary Education Trust Fund (TETFund) under the 2021 National Research Fund (NRF), Nigeria intervention. The authors acknowledge the contribution of Modibbo Adama University, Yola Nigeria and the Chemistry Department of the University where the research was conducted.

## References

- [1] V. Kumar, A. Khan, M. Rabnawaz, Efficient depolymerization of polystyrene with table salt and oxidized copper, *ACS Sustain. Chem. Eng.* 10 (19) (2022) 6493–6502.
- [2] D. Ayre, Technology advancing polymers and polymer composites towards sustainability: a review, *Curr. Opin. Green Sustainable Chem.* 13 (2018) 108–112.
- [3] E.I. Gutierrez-Velasquez, S.N. Monteiro, H.A. Colorado, Characterization of expanded polystyrene waste as binder and coating material, *Case Stud. Constr. Mater.* 16 (2022) e00804.
- [4] N. Mehmandost, M.L. Soriano, R. Lucena, N. Goudarzi, M.A. Chamjangali, S. Cardenas, Recycled polystyrene-cotton composites, giving a second life to plastic residues for environmental remediation, *J. Environ. Chem. Eng.* 7 (5) (2019) 103424.
- [5] S. Agyeman, N.K. Obeng-Ahenkora, S. Assiamah, G. Twumasi, Exploiting recycled plastic waste as an alternative binder for paving blocks production, *Case Stud. Constr. Mater.* 11 (2019) e00246.
- [6] I.M. Maafa, Pyrolysis of polystyrene waste: a review, *Polymers* 13 (2) (2021) 225.
- [7] C. Wang, H. Wu, C. Li, Hysteresis and damping properties of steel and polypropylene fiber reinforced recycled aggregate concrete under uniaxial low-cycle loadings, *Construct. Build. Mater.* 319 (2022) 126191.
- [8] C. Wang, J. Xiao, W. Liu, Z. Ma, Unloading and reloading stress-strain relationship of recycled aggregate concrete reinforced with steel/polypropylene fibers under uniaxial low-cycle loadings, *Cement Concr. Compos.* 131 (2022) 104597.
- [9] J.M. Orts, J. Parrado, J.A. Pascual, A. Orts, J. Cuartero, M. Tejada, M. Ros, Polyurethane foam residue biodegradation through the *Tenebrio molitor* digestive tract: microbial communities and enzymatic activity, *Polymers* 15 (1) (2023) 204.
- [10] S.K. Adhikary, D.K. Ashish, Turning waste expanded polystyrene into lightweight aggregate: towards sustainable construction industry, *Sci. Total Environ.* 837 (2022) 155852.
- [11] R. de Sousa Cunha, G.D. Mumbach, R.A.F. Machado, A. Bolzan, A comprehensive investigation of waste expanded polystyrene recycling by dissolution technique combined with nanoprecipitation, *Environ. Nanotechnol. Monit. Manag.* 16 (2021) 100470.
- [12] G.D. Mumbach, A. Bolzan, R.A.F. Machado, A closed-loop process design for recycling expanded polystyrene waste by dissolution and polymerization, *Polymer* 209 (2020) 122940.
- [13] A.G. Adeniyi, S.A. Abdulkareem, J.O. Ighalo, D.V. Onifade, S.A. Adeoye, A.E. Sampson, Morphological and thermal properties of polystyrene composite reinforced with biochar from elephant grass (*Pennisetum purpureum*), *J. Thermoplast. Compos. Mater.* 35 (10) (2022) 1532–1547.
- [14] M. McCrary-Dennis, M.J. Uddin, O.I. Okoli, Synthesis and characterization of polystyrene carbon nanotube nanocomposite for utilization in the displaced foam dispersion methodology, *Compos. B Eng.* 98 (2016) 484–495.
- [15] S.A. Osemeahon, J.T. Barminas, A.L. Jang, Development of Waste Polystyrene as a binder for emulsion paint formulation II: effect of different types of Solvent, *Journal of Environmental Science, Toxicology and Food Technology* 5 (4) (2013) 1–7.
- [16] N. Saha, S. Banivaheb, M.T. Reza, Towards solvothermal upcycling of mixed plastic wastes: depolymerization pathways of waste plastics in sub- and supercritical toluene, *Energy Convers. Manag.* X 13 (2022) 100158.
- [17] S.A. Osemeahon, I.I. Nkafamiya, O.N. Maitera, A. Akintreinwa, Synthesis and characterization of emulsion paint binder from a copolymer composite of dimethylol urea/polystyrene, *Journal of Polymer and Composites* 3 (2) (2015) 11–21.
- [18] T.A. Bayoumi, M.E. Tawfik, Immobilization of sulfate waste simulate in polymer-cement composite based on recycled expanded polystyrene foam waste: evaluation of the final waste form under freeze-thaw treatment, *Polym. Compos.* 38 (4) (2017) 637–645.
- [19] A. Akinterinwa, S.A. Osemeahon, I.I. Nkafamiya, P.M. Dass, Formulation of emulsion paint from a copolymer composite of dimethylol urea/polystyrene, *Chem. Mater. Res.* 7 (7) (2015) 20–26.
- [20] A. Turner, K.S. Lau, Elemental concentrations and bioaccessibilities in beached plastic foam litter, with particular reference to lead in polyurethane, *Mar. Pollut. Bull.* 112 (1–2) (2016) 265–270.

- [21] Y. Deng, R. Dewil, L. Appels, R. Ansart, J. Baeyens, Q. Kang, Reviewing the thermo-chemical recycling of waste polyurethane foam, *J. Environ. Manag.* 278 (2021) 111527.
- [22] R. Heiran, A. Ghaderian, A. Reghunadhan, F. Sedaghati, S. Thomas, A.H. Haghighi, Glycolysis: an efficient route for recycling of end of life polyurethane foams, *J. Polym. Res.* 28 (2021) 1–19.
- [23] B. Godinho, N. Gama, A. Barros-Timmons, A. Ferreira, Recycling of different types of polyurethane foam wastes via acidolysis to produce polyurethane coatings, *Sustainable Materials and Technologies* 29 (2021) e00330.
- [24] N.V. Gama, A. Ferreira, A. Barros-Timmons, Polyurethane foams: past, present, and future, *Materials* 11 (10) (2018) 1841.
- [25] S.C. Dubey, V. Mishra, A. Sharma, A review on polymer composite with waste material as reinforcement, *Mater. Today: Proc.* 47 (2021) 2846–2851.
- [26] I. Turku, S. Kasala, T. Kärki, Characterization of polystyrene wastes as potential extruded feedstock filament for 3D printing, *Recycling* 3 (4) (2018) 57.
- [27] J.O. Jeong, J.S. Park, Y.M. Lim, Development of styrene-grafted polyurethane by radiation-based techniques, *Materials* 9 (6) (2016) 441.
- [28] G. Moradi, S. Zinadini, L. Rajabi, Development of the tetrathioterephthalate filler incorporated PES nanofiltration membrane with efficient heavy metal ions rejection and superior antifouling properties, *J. Environ. Chem. Eng.* 8 (6) (2020) 104431.
- [29] F. Cisanò, M. Ferrari, Superhydrophobicity and durability in recyclable polymers coating, *Sustainability* 13 (15) (2021) 8244.
- [30] K. Ghosal, C. Nayak, Recent advances in chemical recycling of polyethylene terephthalate waste into value added products for sustainable coating solutions—hope vs. hype, *Materials Advances* 3 (4) (2022) 1974–1992.
- [31] G. Güçlü, Alkyd resins based on waste PET for water-reducible coating applications, *Polym. Bull.* 64 (2010) 739–748.
- [32] C. Gioia, A. Minesso, R. Cavalieri, P. Marchese, A. Celli, M. Colonna, Powder coatings for indoor applications from renewable resources and recycled polymers, *J. Coating Technol. Res.* 12 (2015) 555–562.
- [33] P.V. Schwade, G.O. Schneider, C.K. Santin, T.L.A. de Campos Rocha, Development of paint based on residue of expanded polystyrene: polymeric plasticizer evaluation, in: *Macromolecular Symposia*, vol. 368, 2016, pp. 8–18, 1.
- [34] D. Bellon, W.H. Zamudio, L.C. Tiria, S.M. Durán, I.E. Useche, J. Peña, Effect of expanded polystyrene waste in the creation of waterproofing paint, in: *Journal of Physics: Conference Series*, vol. 1386, IOP Publishing, 2019 012075. No. 1.
- [35] S.A. Osemeahon, B.J. Dimas, Development of urea formaldehyde and polystyrene waste as copolymer binder for emulsion paint formulation, *J. Toxicol. Environ. Health Sci.* 6 (3) (2014) 75–88.
- [36] M. Salama, A.G. Hassabo, A.A. El-Sayed, T. Salem, C. Popescu, Reinforcement of polypropylene composites based on recycled wool or cotton powders, *J. Nat. Fibers* 14 (6) (2017) 823–836.
- [37] J.J. Kwang Yin, M.C. Yew, M.K. Yew, L.H. Saw, Preparation of intumescent fire protective coating for fire rated timber door, *Coatings* 9 (11) (2019) 738.
- [38] M.C. Yew, N.H. Ramli Sulong, M.K. Yew, M.A. Amalina, M.R. Johan, Investigation on solvent-borne intumescent flame-retardant coatings for steel, *Mater. Res. Innovat.* 18 (sup6) (2014) S6–S384.
- [39] Z. Yu, Y. Bai, J.H. Wang, Y. Li, Effects of functional additives on structure and properties of polycarbonate-based composites filled with hybrid chopped carbon fiber/graphene nanoplatelet fillers, *ES Energy & Environment* 12 (2) (2021) 66–76.
- [40] R. Ramos-Olmos, E. Rogel-Hernandez, L.Z. Flores-Lopez, S.W. Lin, H. Espinoza-Gomez, Synthesis and characterization of asymmetric ultrafiltration membrane made with recycled polystyrene foam and different additives, *J. Chil. Chem. Soc.* 53 (4) (2008) 1705–1708.
- [41] D. Chauhan, G. Agrawal, S. Deshmukh, S.S. Roy, R. Priyadarshini, Biofilm formation by *Exiguobacterium* sp. DR11 and DR14 alter polystyrene surface properties and initiate biodegradation, *RSC Adv.* 8 (66) (2018) 37590–37599.
- [42] C. Wang, C. Ma, C. Mu, W. Lin, Tailor-made zwitterionic polyurethane coatings: microstructure, mechanical property and their antimicrobial performance, *RSC Adv.* 7 (44) (2017) 27522–27529.
- [43] V. Chavan, J. Anandraj, G.M. Joshi, M.T. Cuberes, Structure, morphology and electrical properties of graphene oxide: CuBiS reinforced polystyrene hybrid nanocomposites, *J. Mater. Sci. Mater. Electron.* 28 (2017) 16415–16425.
- [44] A.K. Chaudhary, R.P. Vijayakumar, Studies on biological degradation of polystyrene by pure fungal cultures, *Environ. Dev. Sustain.* 22 (2020) 4495–4508.
- [45] M. Zahra, H. Ullah, M. Javed, S. Iqbal, J. Ali, H. Alrbyawi, N. Alwadai, B.I. Basha, A. Waseem, S. Sarfraz, A. Amjad, Synthesis and characterization of polyurethane/zinc oxide nanocomposites with improved thermal and mechanical properties, *Inorg. Chem. Commun.* 144 (2022) 109916.
- [46] R.C.M. Dias, A.M. Góes, R. Serakides, E. Ayres, R.L. Oréface, Porous biodegradable polyurethane nanocomposites: preparation, characterization, and biocompatibility tests, *Mater. Res.* 13 (2010) 211–218.
- [47] D. Sun, Y. Zhang, Preparation of fast-drying waterborne nano-complex traffic-marking paint, *J. Coating Technol. Res.* 9 (2012) 151–156.
- [48] R. Selvasembian, W. Gwenzi, N. Chaukura, S. Mthembu, Recent advances in the polyurethane-based adsorbents for the decontamination of hazardous wastewater pollutants, *J. Hazard Mater.* 417 (2021) 125960.
- [49] R.K. Dhall, Advances in edible coatings for fresh fruits and vegetables: a review, *Crit. Rev. Food Sci. Nutr.* 53 (5) (2013) 435–450.
- [50] N.W. Khun, E. Liu, Tribological behavior of polyurethane immersed in acidic solution, *Tribol. Trans.* 55 (4) (2012) 401–408.